JMEPEG (2011) 20:48–56
DOI: 10.1007/s11665-010-9659-4

1059-9495/$19.00

Thermal Modeling of Direct Digital Melt-Deposition Processes

K.P. Cooper and S.G. Lambrakos

(Submitted March 8, 2010)

Additive manufacturing involves creating three-dimensional (3D) objects by depositing materials layer-by-layer. The freeform nature of the method permits the production of components with complex geometry. Deposition processes provide one more capability, which is the addition of multiple materials in a discrete manner to create "heterogeneous" objects with locally controlled composition and microstructure. The result is direct digital manufacturing (DDM) by which dissimilar materials are added voxel-by-voxel (a voxel is volumetric pixel) following a predetermined tool-path. A typical example is functionally gradient material such as a gear with a tough core and a wear-resistant surface. The inherent complexity of DDM processes is such that process modeling based on direct physics-based theory is difficult, especially due to a lack of temperature-dependent thermophysical properties and particularly when dealing with melt-deposition processes. In order to overcome this difficulty, an inverse problem approach is proposed for the development of thermal models that can represent multi-material, direct digital melt deposition. This approach is based on the construction of a numerical-algorithmic framework for modeling anisotropic diffusivity such as that which would occur during energy deposition within a heterogeneous workpiece. This framework consists of path-weighted integral formulations of heat diffusion according to spatial variations in material composition and requires consideration of parameter sensitivity issues.

Keywords melt deposition, microstructure, solidification, thermal modeling

1. Introduction

A promising research direction in manufacturing science is to develop the concept of a "universal machine" for production. Such a machine could achieve the full realization of virtual prototyping and "Art-to-Part" concepts. It could change the economics of production. Direct digital manufacturing (DDM) could be the answer for a universal manufacturing system. DDM is additive manufacturing with digital control. A DDM-based "universal machine" could offer (1) precision control over multiple material deposition and multiple production length scales, (2) in situ part integrity evaluation and compliance certification, and (3) close coupling of design with fabrication processes for fewer errors in translation and interpretation. It makes possible the fabrication of materials and structures with local control of properties. Such a capability will enable the production of unusual materials and structures. Several direct deposition processes can be adapted for DDM. Processes such as those involving melt deposition can be adapted to produce composite or heterogeneous metallic objects. However, there are challenges associated with multi-material deposition. One challenge is the understanding of localized thermal fields, their influence on localized physical characteristics, and their cumulative effect on the function or behavior of the final product. In order to advance this understanding, thermal modeling of direct digital melt deposition is proposed.

K.P. Cooper and **S.G. Lambrakos**, Materials Science and Technology Division, Naval Research Laboratory, 4555 Overlook Ave., SW, Washington, DC 20375. Contact e-mail: lambrakos@anvil.nrl.navy.mil.

2. A New Way of Making Things

2.1 Additive or Direct Manufacturing

Additive manufacturing encompasses a range of processes that fabricate objects, structures, parts, and components layer-by-layer from the bottom-up (Ref 1). Starting from a CAD solid model, a sliced file is created, which is fed into a layer additive build machine, which produces a physical replica of the CAD model. An advantage of such an approach is the ability to produce objects without part-specific tooling or human intervention, and with complex internal and external geometries, which are not possible by conventional processes such as machining (subtractive), casting, or molding. Direct manufacturing is not suitable for mass production, but is ideal for mass customization. It is a revolutionary approach to manufacturing.

Laser or e-beam melt-deposition techniques are examples of additive or direct deposition processes for metals. A single material in powder or wire form is added to a melt pool formed by a laser or e-beam. Following a predetermined beam path, a "homogeneous" or single-material three-dimensional (3D) structure is built. A schematic of the laser melt-deposition process is shown in Fig. 1(a). A component being made by laser melt deposition is shown in Fig. 1(b) (Ref 2).

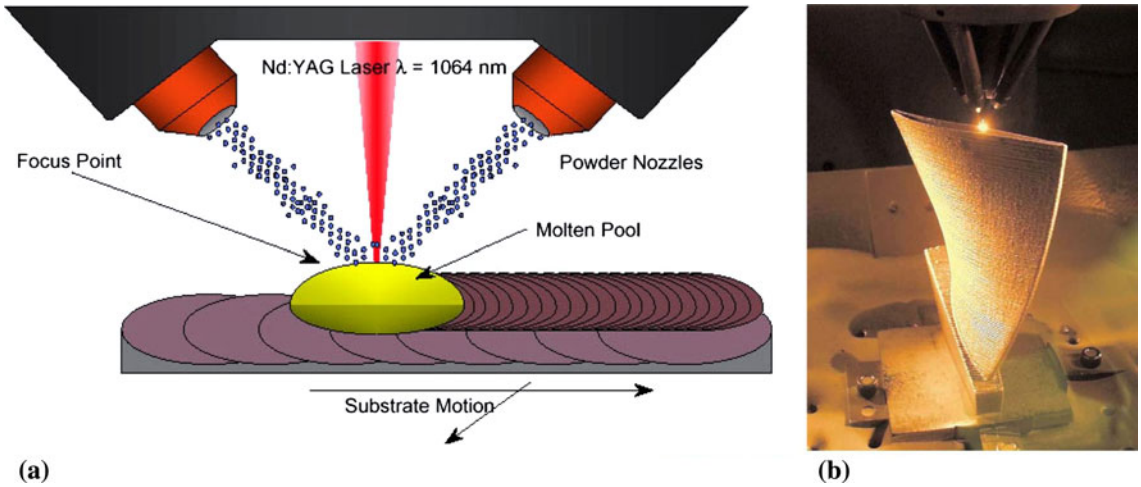

Fig. 1 (a) Schematic of laser melt-deposition process. (b) A turbine blade being made by laser melt deposition (Ref 2). Close examination of the blade surface shows ripples made by layering

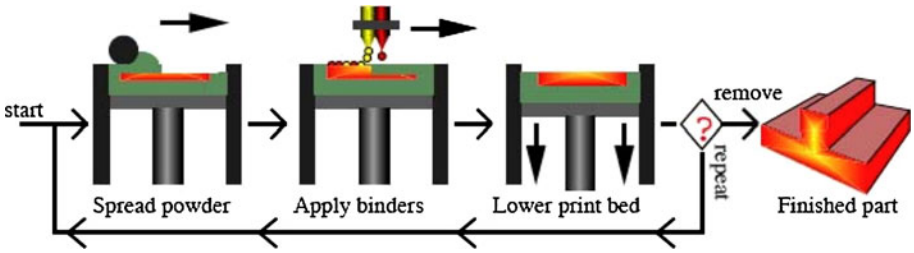

Fig. 2 Schematic diagram showing the DDM concept. The illustration is of multi-material 3D printing (Ref 3)

2.2 Direct Digital Manufacturing

Direct digital manufacturing (DDM) is the method to build objects by digitally controlling highly localized and incremental processing. It involves point-by-point or voxel-by-voxel deposition of material and/or energy. The aim is to produce a unique set of attributes for each voxel (volumetric pixel) or location within the object. If more than one material are added during direct melt deposition or other deposition processes such as 3D printing, then a multi-material, then "heterogeneous" 3D structure can be built. A schematic diagram illustrating the DDM concept is shown in Fig. 2. The illustration is of multi-material 3D printing (Ref 3), but it could equally apply to other deposition processes.

Since it is possible to deposit dissimilar materials in a discrete, incremental manner, it is possible to control the composition and, hence, the physical characteristics at specific locations in the build. If it is possible to control the chemistry of each voxel, then it is possible to control the material properties of each voxel. In addition to localized deposition of material, digital control also allows no deposition or creation of voids. Localized control of voids will enable the fabrication of porous structures of any design. An example is a poro-vascular composite structure. The collective effect of such localized control would be the synthesis of a material or structure that is "unnatural" or unusual. In other words, DDM is the creation of digital materials and structures. The capability of having digital, point-by-point control significantly opens up the material and structure design space to concepts never before considered. It will provide designers more options to push material and component performance and to create materials with properties never imagined. The DDM makes possible discovery of new compounds and materials through computation material science exercises, new physical geometries derived through computation or simulation, and artificial or "uncompromising" materials and structures such as metamaterials. The path to DDM lies in being able to manufacture "things" which *cannot be made in any other way* and give a system-level capability that *cannot be achieved in any other way.*

In order to implement DDM, digitally driven machines will need to be designed for additive fabrication of heterogeneous materials and components *with spatial control of properties*. Composition, macrostructure, microstructure, and texture are some of the properties that can be locally controlled. Essentially, DDM provides a capability to create a new class of materials. Why spatial control of properties? Through spatial control of composition, it is possible to achieve graded yield strength, graded modulus, and compressive regions for fatigue resistance in metals. Through spatial control of macrostructure, it is possible to achieve zero thermal expansion materials, negative Poisson's ratio structures, and foam structures in metals. Through spatial control of texture, it is possible to achieve epitaxial or directional growth, especially of single crystals, and to achieve "pre-trained" shape memory effects in alloys. The DDM allows real control and tailoring of

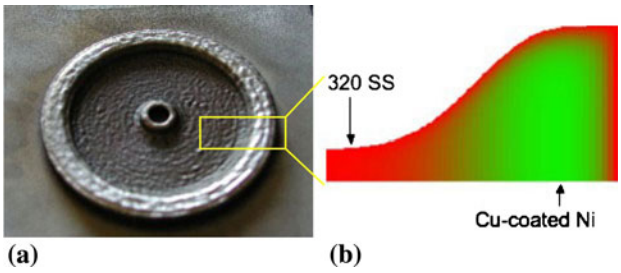

Fig. 3 (a) Graded stainless steel flywheel made by multi-material LENS™ process (Ref 4). (b) Designed composition gradient in cross-section

composition and microstructures. The DDM makes it possible to achieve tunable electronic, magnetic, optical, and mechanical properties and functionalities in materials.

2.3 Direct Digital Melt Deposition

Through multi-material melt additive processes, it is possible to create geometrically complex metallic components while varying the alloy composition in a controlled manner. This permits tailoring of material properties to specific functional requirements. It is possible to fabricate components that contain both discrete and gradual change in alloy composition. This class of materials is called functionally gradient materials or FGMs. FGMs can have alloy composition changes gradually from one material to another or at discrete points in the structure. Thus, it is possible to achieve continuous or discrete gradations in structural and functional properties in DDM materials. An example where performance enhancement via FGM can possibly be achieved is the rotary drill bit. Conceivably, the rotary drill bit can be designed and manufactured in a single operation for both endurance and drilling rate by tailoring *in space* the constituents for both ductile material for endurance and hard abrasive surface material for drilling performance. The drill bit could be made of graded WC/Co, with more WC on the working surfaces for greater erosion resistance and more Co in regions of expected fracture to increase ductility.

An example of a graded stainless steel flywheel made by a DDM process is shown in Fig. 3(a). A schematic representation of the composition variations within the flywheel cross section is shown in Fig. 3(b). The flywheel was made by the LENS™ (laser-engineered net-shaping) process (Ref 4). Another example is the hard-faced down-hole tooling shown in Fig. 4(a) with a wear-resistant graded metal matrix composite surface shown in Fig. 4(b). The down-hole tooling was made by the DMD™ (direct metal deposition) process using multiple powder feeders (Ref 5). The DMD process uses active feedback control, which gives better control on shape and dimension tolerance, and a five-axis moving head allowing deposition through a single setup. Both LENS and DMD are laser deposition processes. These examples demonstrate obtaining gradient microstructures using the direct digital melt-deposition process. Gradient microstructures avoid sharp interfaces that can occur in normal coating processes such as plasma deposition. Gradient microstructures ensure a metallurgical bond, while coatings are prone to delamination and spalling.

In addition to gradient compositions and microstructures, it may be possible to build 3D structures and components with localized differences in microstructure. For example, ferritic

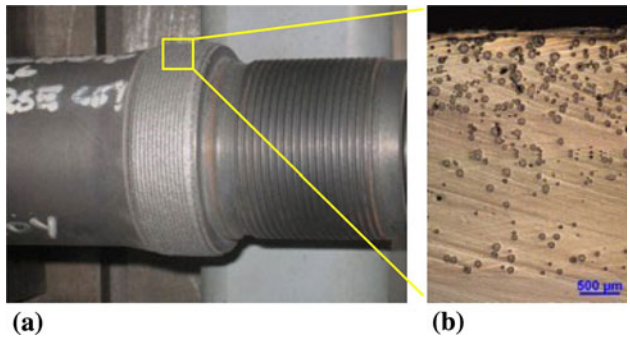

Fig. 4 (a) Hard faced down hole tooling (Ref 5). (b) Graded metal matrix composite surface

and martensitic microstructures in steels arranged in a checkerboard fashion are shown schematically in Fig. 5(a), or crystalline and amorphous phases arranged in a lamellar fashion are shown schematically in Fig. 5(b). These are hypothetical examples and not meant to suggest a material of practical value, but merely to illustrate a point, that is, the capability of DDM to produce digital materials. Obviously, in order to achieve such precision in microstructure control as illustrated in Fig. 5, several issues are raised. Theoretically, it should be feasible to generate any desired microstructure at any location in the build by adding material of certain composition at that location. While material chemistry can imply that a certain microstructure will most likely form, microstructural evolution will depend on many processing factors operating during both molten and solidification stages. The prevailing thermodynamics and kinetics of solidification and phase transformation will control the final microstructure. Other factors that will have to be considered are the resolution, precision and accuracy of deposition, and the resultant microstructure.

3. Basic Research Challenges

Direct digital manufacturing provides a method to create heterogeneous or multi-material objects of any conceivable design. DDM is also capable of making objects with moving parts, e.g., using sacrificial or fugitive materials. Furthermore, when combined with other processes, it may be possible to produce multi-component devices and even engineered systems. However, before DDM becomes a staple for new manufacturing or a key part of a "universal" machine capable of producing wondrous objects, there are several basic research challenges that need to be met. From a processing point of view, digital representations and algorithms will need to be created to enable compilation into an optimized process plan from engineering designs. In other words, the heterogeneous material CAD model will need to be translated to generate multimaterial deposition pathways for building the heterogeneous physical object. In view of the fact that generating single material tool-paths is non-trivial, it follows that generating multi-material tool-paths will be quite challenging. Another challenge would be to develop methodologies for spatial control of properties such as composition, macrostructure, and texture. This will require discovering innovative methods to influence the evolution of localized microstructures.

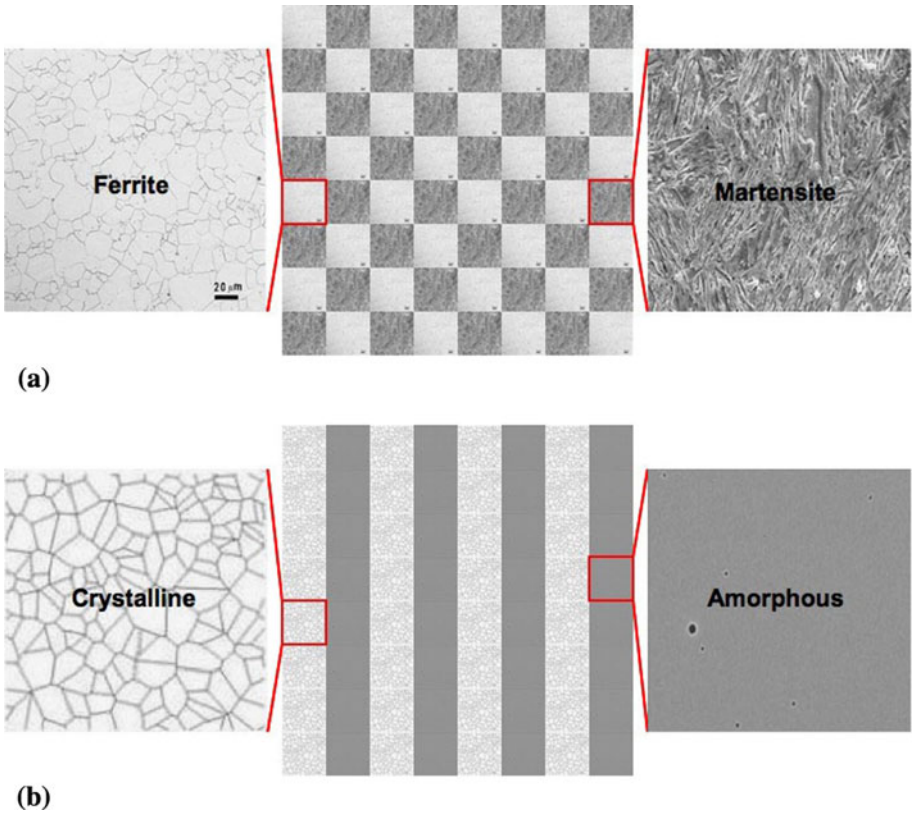

Fig. 5 Hypothetical digital materials produced by DDM. (a) Ferrite + martensite checkerboard microstructure. (b) Crystalline + amorphous lamellar microstructure

For example, using appropriately oriented crystalline seeds to influence texture. In addition to local composition control, it may also be possible to control the amount of heat deposition or energy density, locally. The principles for dissimilar material deposition need to be determined. In metallic systems, not all metals may be compatible for multi-material deposition. Studies are needed to understand the fundamentals of digital manufacturing. In the case of direct digital melt-deposition, it would be useful to understand microstructure evolution, diffusion effects, phase transformations, interfacial behavior and other physical phenomena. A key to understanding microstructure evolution is to determine thermal fields in and around the melt pool, melt temperatures, melt-pool size and shape, fluid flow fields, cooling rates, and temperature histories at various locations in the build. In what follows, a first attempt to develop a general approach for thermal modeling of multi-material melt-deposition processes is presented.

4. Thermal Modeling of Direct Digital Melt-Deposition Processes

4.1 Definition of Inverse Melt-Deposition Problem

Thermal modeling of melt-deposition processes using direct methods is problematic because of a dearth of temperature-dependent thermo-physical properties. In order to overcome this problem, the inverse method approach is extended to model melt-deposition processes (Ref 6, 7). The inverse problem concerning analysis of physical processes, in general, and the inverse heat transfer problem, in particular, may be stated formally in terms of source functions (or input quantities) and multidimensional fields (output quantities). The statement of the inverse problem given here is focused on aspects of the inverse heat deposition problem related to the determination of heat fluxes that can be extended for the modeling of melt-deposition processes. In general, the formulation of a heat conductive system occupying an open-bounded domain Ω with an outer boundary S_o and an inner boundary S_i involves the parabolic equation,

$$\frac{\partial T(\hat{x},t)}{\partial t} = \nabla \cdot (\kappa(\hat{x},t)\nabla T(\hat{x},t)) \qquad \text{(Eq 1a)}$$

for $T(\hat{x},t)$ in $\Omega \times (0,\ t_f)$, with initial condition $T(\hat{x},0) = T_0(\hat{x})$ in Ω, and heat flux exchanges through the outer and inner boundaries S_o and S_i as follows:

$$-\kappa(\hat{x},t)\frac{\partial T(\hat{x},t)}{\partial n_{S_o}} = c(\hat{x},t)(T(\hat{x},t) - T_a(\hat{x},t)) \qquad \text{(Eq 1b)}$$

on $S_o \times (0,\ t_f)$, and

$$-\kappa(\hat{x},t)\frac{\partial T(\hat{x},t)}{\partial n_{S_i}} = q(\hat{x},t) \qquad \text{(Eq 1c)}$$

on $S_o \times (0,\ t_f)$. Here $\hat{x} = (x,y,z)$ is the position vector, n_{S_o} and n_{S_i} are the normal vectors onto boundaries S_o and S_i, respectively, t is the time variable, t_f is the final time, $T(\hat{x},t)$ is the temperature field variable, $\kappa(\hat{x},t)$ is the thermal diffusivity field variable, $c(\hat{x},t)$ and $T_a(\hat{x},t)$ are specified functions, and $q(\hat{x},t)$ is the heat flux on the inner boundary S_i.

Determination of the temperature field via solution of Eq 1 defines the direct initial-boundary value problem. The inverse problem considered here is that of effectively reconstructing the heat flux field $q(\hat{x},t)$ on the inner and outer boundaries S_i, and the resulting temperature field $T(\hat{x},t)$ for all the time $t \in [0,t_f]$ when S_i and S_o are totally or partially inaccessible. In order to reconstruct the heat flux, information on the temperatures $T(\hat{x}_S,t)$, where $\{\hat{x}_S\} \in S_i,S_o$, is needed and, therefore, must be acquired either experimentally or via direct numerical simulation.

Following the inverse analysis approach, a parametric representation based on a physical model provides a means for the inclusion of information concerning the physical characteristics of a given energy deposition process. It follows then that for heat deposition processes involving the deposition of heat within a bounded region of finite volume, consistent parametric representations of the temperature field are given by,

$$T(\hat{x},t,\kappa) = T_A + \sum_{k=1}^{N_k} T_k(\hat{x},\hat{x}_k,t,\kappa;\alpha_1,\ldots,\alpha_n) \quad \text{and} \quad T(\hat{x}_n^c,t_n^c,\kappa) = T_n^c \qquad \text{(Eq 2)}$$

where the quantity T_A is the ambient temperature of the workpiece and the locations $\hat{x}_{n,}^c$ and temperature values T_n^c specify constraint conditions on the temperature field. The function $T_k(\hat{x},\hat{x}_k,t,\kappa;\alpha_1,\ldots,\alpha_n)$ represents an optimal basis set of functions for given sets of boundary conditions and material properties. The quantities $\hat{x}_k = (x_k,y_k,z_k)$, $k = 1, \ldots, N_k$, are the locations of the elemental source or boundary elements. The sum defined by Eq 2 can for certain systems specify numerical integration over the discrete elements of a distribution of sources or boundary elements. Although heat deposition processes may be characterized by complex coupling between the heat source and workpiece, as well as complex geometries associated with either the workpiece or deposition process, in terms of inverse analysis, the general functional forms of the temperature fields associated with all such processes are within a restricted class of functions, i.e., optimal sets of functions. Accordingly, a sufficiently optimal set of functions is that which contains the analytic solutions to heat conduction equation for a finite set of boundary conditions. A parameterization based on this set is both sufficiently general and convenient relative to optimization.

The formal procedure underlying the inverse method considered in this article entails the adjustment of the temperature field defined over the entire spatial region of the sample volume at a given time t. This approach defines an optimization procedure where the temperature field spanning the spatial region of the sample volume is adopted as the quantity to be optimized. The constraint conditions are imposed on the temperature field spanning the bounded spatial domain of the workpiece by minimization of the value of the objective functions defined by,

$$Z_T = \sum_{n=1}^{N} w_n \left(T(\hat{x}_n^c,t_n^c,\kappa) - T_n^c\right)^2 \qquad \text{(Eq 3)}$$

where T_n^c is the target temperature for position $\hat{x}_n^c = (x_n^c,y_n^c,z_n^c)$.

Before proceeding further, it is significant to note the following. First, the general trend features of heat deposition processes are such that the construction of a complete basis set of functions $T_k(\hat{x},\hat{x}_k,t,\kappa;\alpha_1,\ldots,\alpha_n)$ making up a linear combination of the form defined by Eq 2 for representation of the associated temperature field is well defined and readily achievable. Second, for heat deposition processes, characteristics of the temperature field are poorly correlated to characteristics of the energy source. The characteristics of the temperature field, which are associated with these processes, however, are strongly coupled only to inner boundaries on this field, e.g., the solidification boundary. This property follows from the low-pass spatial filtering property of the basis functions $T_k(\hat{x},\hat{x}_k,t,\kappa;\alpha_1,\ldots,\alpha_n)$, whose general forms are consistent with the dominant trend features of heat deposition processes. Third, given a consistent set of basis functions, the temperature field associated with a heat deposition process is completely specified by the shape and temperature distribution of a given inner boundary on the domain of the temperature field; the diffusivity κ; speed of deposition V; and spatial dimensions, e.g., thickness D, of the workpiece. Fourth, the shape and temperature distribution of a specified inner boundary S_i is determined by the rate of energy deposited on the surface of the workpiece and the strength of coupling of the energy source to the workpiece. Furthermore, finally, in view of the fact that an inner boundary S_i is defined by its shape and the distribution of temperatures on its surface $T(\hat{x}_S)$, it follows that one can define a multidimensional temperature field given by $T(\hat{x},\kappa,V,D,T(\hat{x}_S),\ \hat{x}_S \in S_i)$.

The existence of a convenient and general parameterization of inner boundary surfaces, $T(\hat{x}_S),\ \hat{x}_S \in S_i$, bounding the temperature fields associated with heat deposition processes follows from the fact that all heat deposition processes are characterized by thermal and energy deposition profiles whose general form can be represented by a small class of geometric shapes. Accordingly, the observed volumetric distributions of energy from all types of heat deposition processes, within the inner boundary S_i of their associated temperature fields, can be represented by linear combinations of basis functions that are within the class of generalized functions that are defined by the dominant trend features associated with volumetric energy deposition. These generalized functions provide for the construction of a relatively optimal and general parametric representation $T(\hat{x},\kappa,V,D,T_s(\hat{x}_S),\ \hat{x}_S \in S_i,S_o)$ for inverse analysis of heat deposition processes that are characterized by drop-by-drop liquid-metal deposition. In doing so, the inverse problem defined by the mapping,

$$C(\hat{x}_k) \mapsto T(\hat{x}), \qquad \text{(Eq 4)}$$

where $C(\hat{x}_k)$ is the energy source function, and is replaced by the inverse problem defined by the mapping,

$$C(\hat{x}_k),\kappa \mapsto S_i,S_o \mapsto T(\hat{x}). \qquad \text{(Eq 5)}$$

Following the same arguments, the definition of the inverse heat deposition problem as given above can be extended to include systems that are characterized by incomplete information concerning the diffusivity function κ. This would include any nonlinear dependence of κ on temperature, and for applications involving drop-by-drop liquid-metal deposition, spatial dependence of κ. This follows in view of the fact that Eq 5 implies the existance of a weighted space averaged diffusivity and provides a foundation for parameterization using path-weighted diffussivity functions.

Given an inverse analysis formulation that is defined by the sequence of mappings Eq 5, relatively interesting sensitivity

issues which follow are observed. The mathematical properties underlying these sensitivity issues are the same as those reponsible for the ill disposition of many inverse analysis procedures based on the mapping Eq 4. That is to say, those filter properties of diffusion processes, which tend to make the temperature field $T(\hat{x})$ insensitive to details of the shape of the source distribution $C(\hat{x}_k)$, tend to make $T(\hat{x})$ insensitive to details of the shapes of S_i and S_o. This insensitivity to details of the shapes of S_i and S_o, e.g., the shape of the solidification boundary, implies that a general parametric representation of the inner and outer boundaries can in principle be formulated in terms of a reasonably convenient mathematical form.

4.2 Parameterizations Using Analytical Basis Functions and Path-Weighted Diffusivity Functions

As demonstrated in previous studies, the parametric representation of the form given by Eq 2 is sufficiently flexible for construction of temperature fields associated with heat deposition processes where source and workpiece characteristics are relatively simple. It is significant to note, however, that many energy deposition processes are characterized by volumetric coupling of the energy source and associated diffusion patterns that are relatively complex. Accordingly, it would be advantageous to extend the adjustability of the mapping defined by Eq 2 for the purpose of representing more complex diffusion patterns. As shown previously, the adjustability of the parameterization can be extended by adopting basis functions whose spatial distributions are spatially modulated. Among the many different possible types of spatial modulation, which can be applied are those whose application produces diffusion patterns that are directionally or path weighted. The extension of the mapping defined by Eq 2 for the inclusion of spatial modulation can be expressed by

$$T(\hat{x}, t, \kappa, V, D, T_s(\hat{x}_S),\ \hat{x}_S \in S_i, S_o) = T(\hat{x}, t, \kappa_m(\hat{x}), C(\hat{x}_k), \hat{x}_k, t_k, \Delta t, N_t, N_k, V_k). \quad \text{(Eq 6)}$$

Given the parameterization framework defined by Eq 6, it follows that a consistent representation, in terms of basis functions, of the temperature field associated with spatially modulated heat diffusion patterns is,

$$T(\hat{x},t) = T_A + \sum_{k=1}^{N_k}\sum_{n=1}^{N_t} C(\hat{x}_k, n\Delta t) F(\hat{x}, \hat{x}_k, n\Delta t, \kappa_m(\hat{x}))\delta(n\Delta t - t_k) \quad \text{(Eq 7)}$$

where

$$F(\hat{x}, \hat{x}_k, t, \kappa_m(\hat{x})) = \frac{1}{t}\exp\left[-\frac{(x-x_k)^2 + (y-y_k)^2}{4\kappa_m(\hat{x})t}\right] \times \left\{1 + 2\sum_{m=1}^{\infty}\exp\left[-\frac{\kappa_m(\hat{x})m^2\pi^2 t}{l^2}\right] \times \cos\left[\frac{m\pi z}{l}\right]\cos\left[\frac{m\pi z_k}{l}\right]\right\}, \quad \text{(Eq 8)}$$

$t = N_t\Delta t$ and $\delta(t)$ is the Dirac delta function representing the instantaneous deposition at locations $\hat{x}_k = (x_k, y_k, z_k)$ at times $t = t_k$. The speed of energy deposition V_k, which is an implicit function of position on the surface of the workpiece, is given by

$$V_k = \frac{x_k - x_{k-1}}{t_k - t_{k-1}}. \quad \text{(Eq 9)}$$

Referring to Eq 7-9, it is to be noted that spatial modulation of the diffusion field is through functional dependence on the generalized diffusivity function $\kappa_m(\hat{x})$ and the adjustable parameters Δt, N_t, N_k and V_k. Consistent with the generalized mapping represented by Eq 6, the parameter V_k, which can be a function of the discrete index k, can assume values that are in general not equal to the speed of the energy source V relative to the workpiece. Accordingly, the procedure for inverse analysis defined by Eq 7-9 entails adjustment of the parameters $C(\hat{x}_k, n\Delta t), \hat{x}_k, \Delta t$ and V_k defined over the entire spatial region of the workpiece.

At this stage it is appropriate to establish interpretation of the parameterizations expressed by the basis functions defined by Eq 7-9. First, it must be emphasized that the primary set of parameters for system representation, which are uniquely defined, are the quantities $(V, D, \kappa, T_s(\hat{x}_S),\ \hat{x}_S \in S_i, S_o)$. Second, the weighted sums of basis functions defined by Eq 7-9 establish a set of parameters, which are not uniquely defined, but establish the mapping expressed by Eq 6. Accordingly, the mapping from one set of parameters to another, defined by Eq 6, provides foundation for a general framework for spatial modulation of heat diffusion patterns for convenient construction of the temperature field $T(\hat{x}, t, V, D, \kappa, T_s(\hat{x}_S),\ \hat{x}_S \in S_i, S_o)$.

The necessity of a more general and flexible parameterization follows from the specific definition of the inverse heat transfer problem that is considered in this article, and the associated conditions for its application. That is to say, the goal of any inverse analysis following the general procedure considered is construction of a temperature field $T(\hat{x}, t, \kappa, V, D, T_s(\hat{x}_S), \hat{x}_S \in S_i, S_o)$, where the surface distribution of temperatures $T_s(\hat{x}_S), \hat{x}_S \in S_i, S_o$, represents the only constraint condition on the calculated temperature field. Accordingly, parameterizations that are sufficiently flexible and convenient with respect to variation of heat diffusion patterns are required.

In its simplest form $\kappa_m(\hat{x}) = \kappa_0$, a constant value that is approximately equal to the average diffusivity κ of the material of the workpiece. For purposes of establishing the mapping defined by Eq 6, however, $\kappa_m(\hat{x})$ can be generalized to represent a spatially weighted average diffusivity using the expression,

$$\kappa_m(x) = (1 - x/L)\kappa_1 + (x/L)\kappa_2 \quad \text{(Eq 10)}$$

where κ_1, κ_2, and L can in principle be phenomenological adjustable parameters or quantities related to actual material diffusivities and workpiece dimensions. A 2D extension of Eq 10 is given by,

$$\kappa_m(x,y) = \left(1 - \sqrt{x^2+y^2}/L\right)\kappa_1 + \left(\sqrt{x^2+y^2}/L\right)\kappa_2 \quad \text{(Eq 11)}$$

Next, given that a function $\kappa_m(\hat{x})$ has been specified, a general path-dependent weighted average diffusivity can be given by,

$$\langle\kappa_m(r,\theta)\rangle = \frac{1}{r}\int_0^r \kappa(r',\theta)dr' = \frac{1}{r}\sum_{k=1}^{N_k}\kappa(k\Delta r,\theta)\Delta r = \frac{1}{N_k}\sum_{k=1}^{N_k}\kappa(k\Delta r,\theta). \quad \text{(Eq 12)}$$

The functionality expressed by Eq 12 provides a directional path-integral weighting of the heat diffusion pattern. Directional path-integral weighting provides a representation of heat-diffusion trends that can be associated with an anisotropic diffussivity function.

5. Prototype Analysis

In this section, a prototype analysis is described demonstrating the application of the general algorithmic structure presented above to the inverse analysis of layer-by-layer deposition processes. The prototype system is that of the freeform fabrication of a 2D coupon for a system whose thermal diffusivity is a function of position. The model system consists of a sequence of layers, where each layer consists of a distribution of discrete energy sources whose strengths are assigned by the values of the coefficients $C(\hat{x}_k, n\Delta t)$ defined in Eq 7 and are numerically integrated, or summed discretely, at each time step. Each of the discrete energy sources represents a discrete liquid metal droplet of a given volume. The translation speed of the sample relative to the point of liquid metal deposition is assigned implicitly through the time dependence and relative locations of the discrete energy sources, $C(\hat{x}_k, n\Delta t)$. That is to say, a certain number of drops per layer and a certain number of layers as a function of time are specified. The model parameters used for the prototype analysis are listed in Table 1. For purposes of this analysis, the basis function $F(\hat{x}, \hat{x}_k, t, \kappa)$ given by Eq 8 is adopted for calculation of the temperature field. These functions are the solution to the heat conduction equation for a temperature-independent diffusivity and non-conducting boundaries on two surfaces that are separated by a distance l, which will correspond to the thickness of the coupon to be fabricated. Accordingly, it is assumed for this simulation that there is no conduction at the substrate boundary. An additional condition imposed on the model system is that of heat transfer into the ambient environment at the edges of the rectangular coupon being fabricated. This is a realistic assumption for process conditions where droplet-by-droplet deposition occurs within a mold structure consisting of a metal powder composite whose thermal diffusivity is similar to that of the fabricated structure, e.g., rectangular coupon. A constraint condition imposed on the temperature field is that the liquid-solid interface defined by the alloy liquidus temperature is at that of the specific alloy at any given position within the material. Accordingly, the values assigned to the coefficients $C(\hat{x}_k, n\Delta t)$ were such that the average temperature of each discrete droplet was within the range of liquid metal. It is significant to note that other constraint conditions such as melt-pool dimensions and measurements of temperature via thermocouples can also be adopted for assigning values to the coefficients $C(\hat{x}_k, n\Delta t)$. In the present prototype analysis, the layers are deposited one on top of the other by traversing the passes in a zig-zag fashion. Consistent with the filter properties associated with thermal diffusion, each melt bead droplet can be represented by a cube (see Table 1). This follows in view of the fact that the filtering of fine spatial structure due to the dominant trend factor Eq 10 implies that the temperature field is insensitive to details of the shape of the melt bead droplet. It is significant to note, however, that the temperature field is sensitive to the spatial distribution of droplets. The prototype analysis considers calculation of the temperature field at a sampling point within the model structure.

Table 1 Model parameters used to determine thermal fields in layer-by-layer deposition process

Model parameters
Material: Cu-Ni alloy distribution
Diffusivity: Given by Eq 13
Timestep: Δt = 0.005 s
Drop deposited every 5 timesteps
11 drops per layer
Droplet energy content: $C(\hat{x}_k, n\Delta t)$ = 4.0
Droplet volume = $(\Delta l)^3$, Δl = 0.1667 cm

The prototype analysis is characterized by energy deposition within a material having inhomogeneous and anisotropic thermal diffusivity. The system, which consists of a 2D discrete distribution of Cu-Ni alloys of variable relative percentage as a function of position, is described schematically in Fig. 6. This alloy distribution is characteristic of that which would be constructed by drop-by-drop liquid metal deposition of 11 alloys (differing in wt%) being dropped sequentially to build-up a thin wall. The liquidus temperature as a function of relative alloy composition is given in Table 2. A diffusivity function and average liquidus temperature field are constructed according to the 2D discrete distribution of Cu-Ni alloys. Accordingly,

$$\kappa_m(x,y,z) = (1 - x/L)\kappa_1 + (x/L)\kappa_2 \text{ and}$$
$$T_M(x,y,z) = (1 - x/L)T_{M1} + (x/L)T_{M2} \quad \text{(Eq 13)}$$

where $\kappa_1 = 1.136 \times 10^{-4}$ m^2/s, and T_{M1} = 1085 °C, corresponding to pure Copper, and $\kappa_2 = 2.303 \times 10^{-4}$ m^2/s and T_{M2} = 1455 °C, corresponding to pure Nickel. The prototype

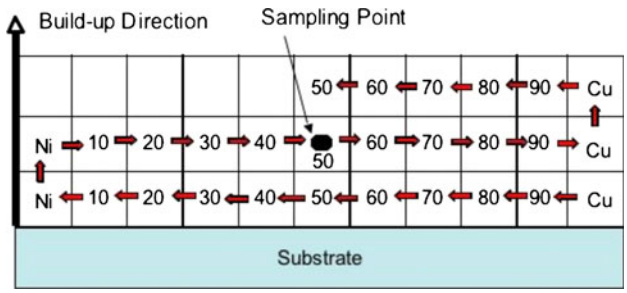

Fig. 6 Schematic representation of drop-by-drop liquid metal deposition process assumed for workpiece construction

Table 2 Liquidus temperature as a function of Cu-Ni alloy composition

Alloy	Liquidus, °C
Pure Cu	1085
Cu-10	1150
Cu-20	1200
Cu-30	1245
Cu-40	1280
Cu-50	1320
Cu-60	1350
Cu-70	1375
Cu-80	1410
Cu-90	1430
Pure Ni	1455

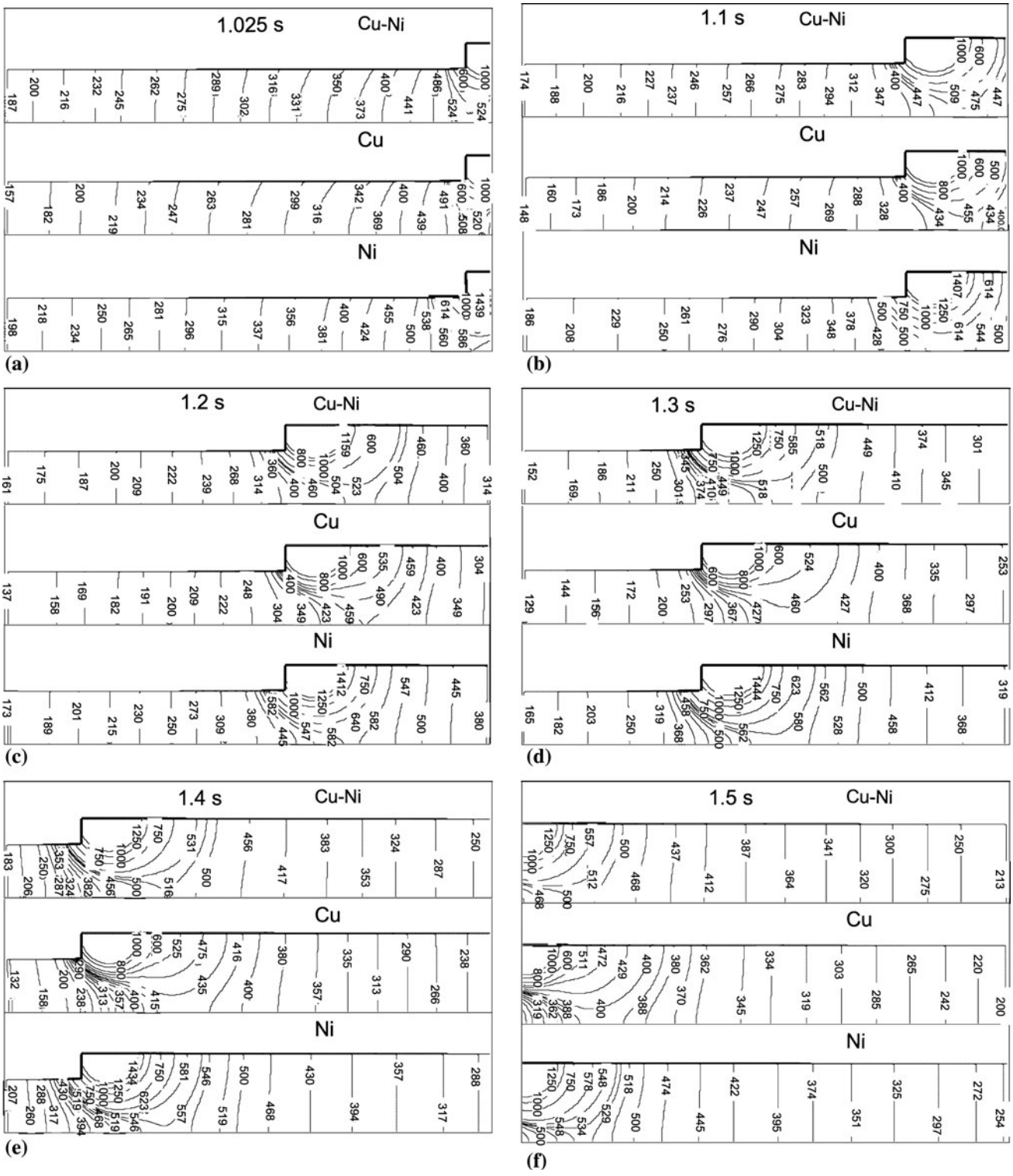

Fig. 7 Two-dimensional temperature distributions (°C) of built structures consisting of Pure Cu, Pure Ni and Cu-Ni alloy composite after deposition of first droplet at (a) 1.025 s, (b) 1.1 s, (c) 1.2 s, (d) 1.3 s, (e) 1.4 s, (f) 1.5 s

analysis that follows consists of temperature field calculations that demonstrate the influence of path-weighted diffusivity on heat diffusion patterns according to adjustment of the various parameters associated with the basis functions defined by Eq 7 through 10.

Considered are calculations of temperature fields that adopt the spatially dependent diffussivity function Eq 13, the constant diffusivities $\kappa_1 = 1.136 \times 10^{-4}$ m^2/s and $\kappa_2 = 2.303 \times 10^{-4}$ m^2/s, corresponding to pure Copper and Nickel, respectively, and adjusted discrete spatial distributions of the effective

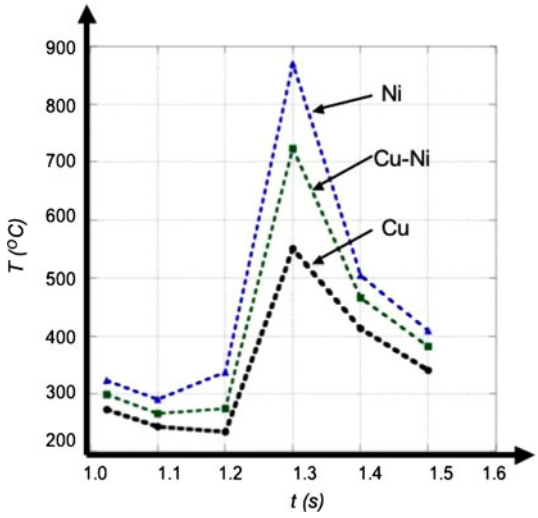

Fig. 8 Temperature histories at sample points within built structures consisting of Pure Cu, Pure Ni, and Cu-Ni alloy composite defined according to Fig. 6

heat source given by Eq 7 so that the calculated cross sections of the solidification boundary satisfy, in principle, experimentally observed solidification patterns or droplets of given volume whose average temperature, which is above liquidus, has been specified. The results of these calculations are shown in Fig. 7 and 8 for the weighted sums of basis functions defined by Eq 7.

The plots in Fig. 7 are of 2D temperature distributions in the built structures for Ni, Cu and Cu-Ni alloys, respectively, at incremental time-steps corresponding to the sequential deposition of molten metal droplets. In addition to differences in peak temperature, due to differences in the melting and liquidus temperatures, differences in melt-pool size and thermal gradient in the solidified structure are observed. Fig. 8 gives the temperature histories at the sample point shown in Fig. 6 within the build structure for Cu, Ni and Cu-Ni alloys as the molten droplets are sequentially deposited. The plots show four trends. An initial slow cooling trend as the previously deposited material cools, a sharp increase in temperature as the droplet deposition approaches the sample point, a rapid drop in temperature as the deposition moves away from the sample point, and a slow drop in temperature as the heat deposition recedes further away. Temperature histories are an indication of the thermal cycles experienced by each voxel of the deposited structure, which will influence microstructure evolution and desired properties. The extent of microstructural modification will depend upon the distribution of the thermal fields and the magnitude of the temperature histories. These factors must be taken into consideration as a heterogeneous structure is built voxel-by-voxel via direct digital melt deposition.

6. Summary

It appears that in metallic systems unusual microstructures with voxel-by-voxel or local control can be produced by direct digital melt deposition. The degree of local control of composition and microstructure will depend upon the thermal response of the material to the incident energy. The modeling objective of this article was to present a preliminary description of general parameterizations of time-dependent temperature fields occurring in drop-by-drop metal deposition processes where there exists inhomogeneous or anisotropic thermal diffusivity. These generalized parameterizations follow from a specific and restricted definition of the inverse heat transfer problem.

Acknowledgment

The authors thank the Office of Naval Research for its support in performing this research.

References

1. K.P. Cooper, Layered Manufacturing: Challenges and Opportunities, *Mater. Res. Soc. Symp. Proc.*, 2003, **758**, p LL1.4.1
2. Sandia National Laboratories, *Advanced Metallurgy*, 2007, https://share.sandia.gov/8700/projects/content.php?cid=50
3. T.R. Jackson, H. Liu, et al., Modeling and Designing Functionally Graded Material Components for Fabrication with Local Composition Control, *Mater. Des.*, 1999, **20**, p 63
4. G.M. Fadel, S. Morvan, et al., *Solid Freeform Fabrication Proceedings*, University of Texas, Austin, TX, 2001, p 553
5. J. Mazumder, University of Michigan, Ann Arbor, MI, 2009, Private Communication
6. K.P. Cooper and S.G. Lambrakos, *Supplemental Proceedings: Vol 1: Fabrication, Materials, Processing and Properties*, TMS, Warrandale, PA, 2009, p 351
7. S.G. Lambrakos and K.P. Cooper, *J. Mater. Eng. Perform.*, 07 Jul 2009, Publ. on-line